



# Effect of water salinity on properties of multipass underwater wet manual metal arc welded joints

Jacek Tomków<sup>1</sup> · Dariusz Fydrych<sup>1</sup> · Jerzy Łabanowski<sup>1</sup>

Received: 10 February 2023 / Accepted: 24 June 2023 / Published online: 10 July 2023  
© The Author(s) 2023

## Abstract

The weldability of steel under the water is limited due to the influence of the environment. Water causes limited visibility, presence of the residual stresses, increasing the cooling rate, and increasing the diffusible hydrogen content in deposited metal, leading to the formation of brittle microstructures in heat-affected zone (HAZ). The paper presents the results of mechanical properties testing of S420G2+M steel welded joints made with covered electrodes in the water with salinity values: 0‰, 7.5‰, and 35‰. The non-destructive tests: ultrasonic (UT) and radiographic (RT), and destructive tests: Vickers HV10 measurements, Charpy impact, and bending and metallographic macro- and microscopic tests were performed. Moreover, the diffusible hydrogen content in deposited metal by the mercury method was measured. It was observed that water salinity has an influence on the stability of the welding arc and the properties of joints. In particular, it was found that increasing the water salinity provides to: decreasing the hardness of HAZ (from 211 HV10 to 193 HV10), increasing the impact strength (from 82.5 to 101.3 J/cm<sup>2</sup>). Additionally, a slight increase in the diffusible hydrogen content in deposited metal (up to 65 ml/100g) was observed. The number of microcracks in the joints decreased with increasing the water salinity.

**Keywords** Underwater wet welding · S420G2+M steel · High-strength low-alloy steel · Manual metal arc welding · Water salinity · Diffusible hydrogen

## 1 Introduction

Each year, the number of marine and offshore structures as pipelines, platforms etc., increases [1, 2]. These structures may undergo failures, which require repairs directly in the water. Underwater welding could reduce the cost of the process by avoiding transport of offshore and marine structures into the air. It also allows to perform processes directly in a water environment, which could be helpful in necessity repairs in a short time [3–6]. There are three main

methods of underwater welding [7, 8]. The first, named dry welding, in which the welding area and the welder are isolated from the surrounding environment [3]. However, there is a necessity to build special, high-cost chambers, which provide limitations of usage of this method. The second of underwater welding methods is local cavity welding. In this method, there is a small chamber, which provide isolation of the welding arc and the welding pool from the water [9]. The diver–welder is in direct contact with the water. Local cavity welding is not so widely used in real applications due to its limited visibility of the welding area. The third and the most often used underwater welding technique is wet welding. The process is carried out with direct contact of the welding area and welding pool with the surrounding environment [10]. In the case of underwater welding, the main problems are as follows [11, 12]: instability of the welding arc, limited visibility, high residual stresses, and high susceptibility to cold cracking. The last one is treated as a main factor in underwater weldability assessment.

Many offshore structures require the usage of high-strength low-alloy (HSLA) steels and ultra-high-strength steel [13–15]. Increasing the mechanical properties of steel allows to reduce

---

Recommended for publication by Commission XII - Arc Welding Processes and Production Systems

---

✉ Jacek Tomków  
jacek.tomkow@pg.edu.pl  
Dariusz Fydrych  
dariusz.fydrych@pg.edu.pl  
Jerzy Łabanowski  
jerzy.labanowski@pg.edu.pl

<sup>1</sup> Faculty of Mechanical Engineering and Ship Technology, Gdańsk University of Technology, Gdańsk, Poland

the cost of structures resulting from reduction of the thickness of elements [16–18]. However, it often leads to decreasing the material weldability [19–21]. Many investigations proved that the quality of underwater joints is lower than in the case of joining in the air. However, recent investigations showed that it is possible to produce similar quality structures [22–24].

Klett et al. [25] proved that increasing welding depth allows to reduce the tendency to cold cracking by reducing the diffusible hydrogen amount in deposited metal. The same could be achieved by changing of welding parameters, which was proved by Fydrych et al. [26]. Increasing the welding heat input may also be a way to improve the quality of HSLA steels' underwater welded structures. Tomków et al. [27] proved that higher heat input allows to reduce the number of cold cracks both in the heat-affected zone (HAZ) and in weld metal. Additional ways to improve the quality of underwater welded structures may be: modifications of welding consumables [28], ultrasonic wave application [11], and temper bead welding (TBW) [29].

However, the mentioned papers did not focus on the type of water. Only 3% of Earth's water is fresh while 97% is saline [30]. There are limited literature proceedings showing influence of water salinity on the underwater welding process and its results. Most of them focused on the influence of the salinity on the diffusible hydrogen content in deposited metal. Kononenko [31] focused on underwater flux-cored arc welding (FCAW). It was proved that increasing the water salinity resulted in decreasing the diffusible hydrogen content in deposited metal. Similar results were observed for underwater wet welding with manual metal arc (MMA) welding by Fydrych and Rogalski [32]. In this study, two states of the water were compared—fresh water and saline Baltic Sea water. It was proved that fresh water as a welding environment generates 59.45 ml/100g hydrogen in deposited metal, compared to 72.32 ml/100g in freshwater. Some important aspects of water salinity were studied by Yushchenko et al. [33]. Firstly, it was confirmed that with the higher water salinity the hydrogen content of weld metal decreases by 5–10% and the oxygen content increases by 5–15%. Authors proved that the additional quantities of potassium, sodium, magnesium, and calcium salts get into the arc gas. The higher concentrations of the mentioned elements in the arc gas change the character of heat transfer to a droplet causing the increase in the degree of its overheating. Higher temperature of droplets resulted in more intensive oxidation, which leads to the metal absorption of hydrogen, since oxygen, while being a surface-active element, blocks the interface and decreases hydrogen solubility. The next aspect investigated by the authors was the influence of water salinity on the stability of the welding arc. According to observed results, welding arc stability in the freshwater is lower than in sea water, which may result in lower quality

**Table 1** Chemical composition of used materials wt. %

| Material  | C    | Mn   | Si   | Ni   | C <sub>eIIW</sub> |
|---|------|------|------|------|-------------------|
| S420G2+M by analysis  | 0.10 | 1.57 | 0.44 | 0.07 | 0.37              |
| E 42 2 1Ni RR 51 electrode in accordance with manufacturer data | 0.05 | 0.50 | 0.45 | 0.30 | -                 |

**Table 2** Mechanical properties of used materials in accordance with manufacturer certificates

| Weld no.                           | Yield point, $R_e$ (MPa) | Tensile strength, $R_m$ (MPa) | Elongation, $A_5$ (%) |
|------------------------------------|--------------------------|-------------------------------|-----------------------|
| S420G2+M                           | 520                      | 612                           | 27.1                  |
| E 42 2 1Ni RR 51 electrode deposit | -                        | At least 540                  | At least 26.0         |

of welded joints. This effect is explained by the presence of dissociated salts. Moreover, increasing the salinity of water provides to increasing the cooling rate of 1.25–1.43 times. It is explained by weakening of the protective role of vapor jacket at sample surface due to the presence of compound HCl in sea water.

Analysis of literature showed that the influence of water salinity on the properties of underwater wet MMA welded joints still needs to be investigated. There are no investigations in the field of multipass butt joints welding with the usage of high-strength low-alloy steel in water with different levels of salinity. Increasing usage of HSLA steels required investigations of their behavior during welding in sea water. The presented paper focused on the three states of water—fresh water, Baltic Sea water, and oceanic water, as representatives for assessment of the effect of water salinity to the properties of underwater welded structures.

## 2 Materials and methods

As a base material (BM) S420G2+M steel plates with dimensions 150 mm × 85 mm × 15 mm were chosen, which is well suited for a harsh environment including seawater. It is used in high-strength oil and offshore structures, mostly in marine drilling and offshore platforms [21]. For welding, MMA welding method was selected due to the most common usage of this process in a water environment. As a filler material, the rutile underwater 4.0-mm diameter electrodes (nearest equivalent E 42 2 1Ni RR 51) were used. The chemical compositions and mechanical properties of used materials are listed in Tables 1 and 2. The chemical

composition of the BM has been tested by emission spectroscopy with a spark excitation method.

For investigations, three levels of water salinity were assumed: fresh water—specimens 1 and 2, the Baltic Sea salinity (which averages 7.5‰)—specimens 3 and 4, and oceanic water (which averages 35‰)—specimens 5 and 6. Six (two for each state of the water) specimens were performed at 0.5 m (20 °C) depth in the underwater welding stand (Fig. 1). The welding parameters were chosen to obtain similar heat input values for the same layers in the range 0.9–1.1 kJ/mm. This range allows to minimize the number of cracks in welded structures, which was proved during preliminary investigations [27].

S420G2+M steel plates were prepared with a “Y groove” (60°, 0.5-mm distance) and were joined by tack welds at the root side before test welding. All specimens were multipass welded with 7 welding passes, in which the last one was wave welded to form a flat weld face. The schematic view of the way of beads arranging during welding is presented in Fig. 2.

All welded joints were subjected to the non-destructive test (NDT)—visual (VT) following requirements of EN ISO 17637:2017 standard, radiographic (RT)

following requirements of EN ISO 5579:2014 standard, and ultrasonic phased array (UTPA) tests following requirements of ISO 13588:2019 standard. For RT, the ANDREX 300-kV X-ray stand was used. Following preliminary investigations, the focal length 700 mm, exposure time 5 min 30 s, voltage 185 kV, and anode current intensity 4.5 mA parameters were chosen. UTPA test was performed using Phasor XS flaw detector, with 16 an element head, with the angle of inclination at 36°. During tests, type A and S imaging were obtained. The aim of these tests was the assessment of the quality of the prepared joints, and selection of the appropriate places for cutting samples for further investigations.

Then, the areas for destructive tests were selected. Samples were cut, ground, polished, and etched (Nital 4%). Performed destructive tests included the following: metallographic macro- and microscopic conducted in accordance with EN ISO 17639:2013, Vickers HV10 hardness measurements following the EN ISO 9015-1:2011, Charpy impact test, and three-point bending test. The Vickers measurements were performed in accordance with the EN ISO 9015-1:2011 using Sinowon V-10 hardness tester with a load of  $F = 98.07$  N (HV10). For Charpy impact test, from each joint, two specimens were cut and performed with V-notch located in the weld. The V-notch has been made with an angle of 45° and a depth of 2 mm. The width and height of the sample were 10 mm. Tests were performed with requirements of the EN ISO 148-1:2017 standard. Two specimens were prepared for a bending test. The criterion of acceptance was defined as a bend angle of 180°. Additionally, the diffusible hydrogen content in deposited metal was determined by mercury measurement method according to ISO 3690:2018 (specimen B). This method is characterized by greater accuracy compared to glycerine method, which also can be used for high hydrogen welding processes [25, 27]. Measurements were conducted in the stand presented in Fig. 3.

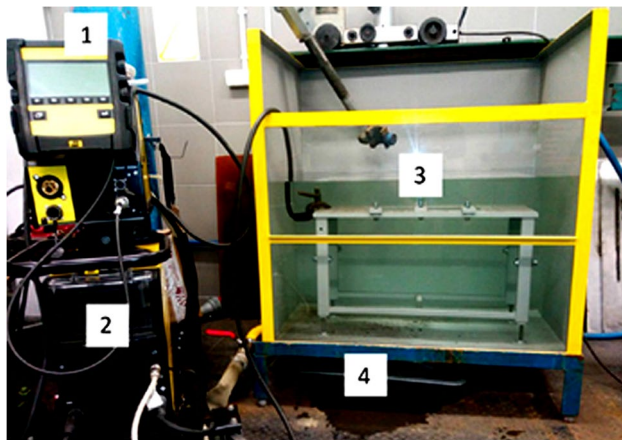


**Fig. 1** Underwater welding stand: (1) control panel, (2) welding power source, (3) welding table, and (4) water tank

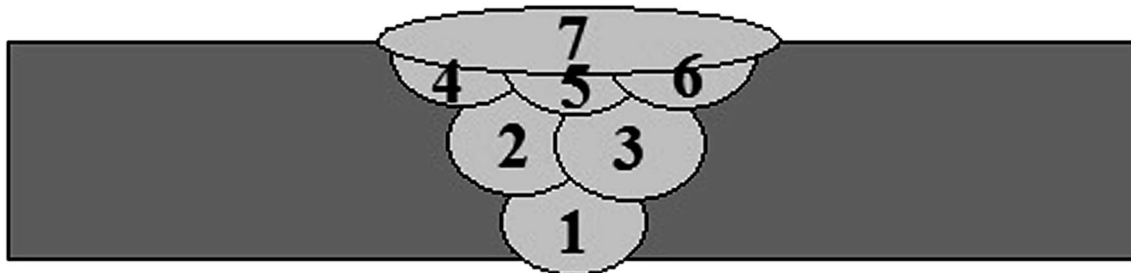


**Fig. 2** Schematic view of way of beads arranging, numbers mean order of welding

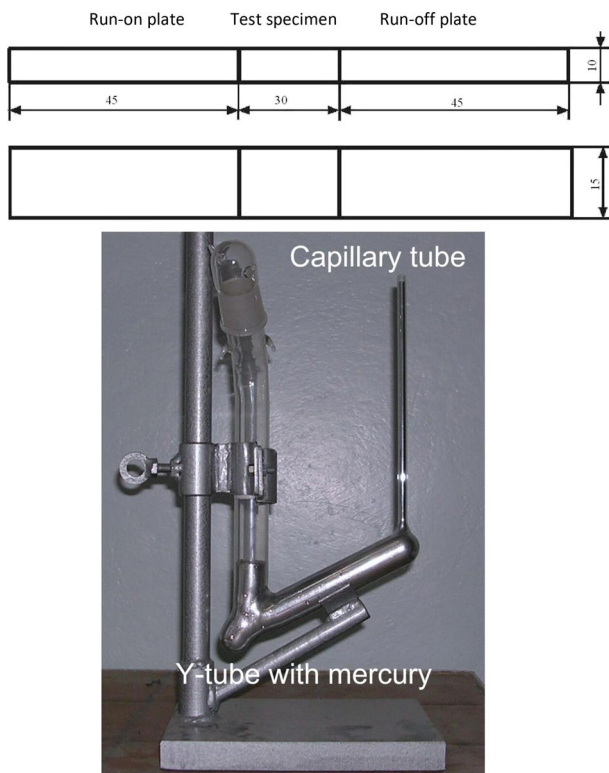


**Fig. 3** Specimen geometry and stand for mercury hydrogen content in deposited metal measurements

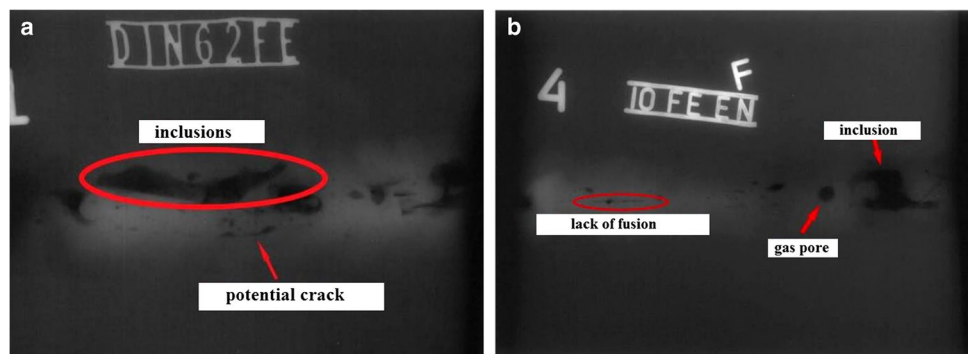
### 3 Results and discussion

During welding, the influence of water salinity on the process was observed. Increasing the water salinity causes higher stability of the welding arc, which confirmed previous investigations [31]. Also, the differences in electrode behavior was observed—they melted more stable in water characterized by higher salinity.

#### 3.1 Non-destructive tests

During VT, some of the typical underwater welding imperfections [34, 35] as undercuts and porosity were

**Fig. 4** Exemplary radiographs: **a** specimen 2—fresh water and **b** specimen 4—Baltic Sea water



observed. In the next step, the RT test was performed (Fig. 4). The presence of internal imperfections was detected in specimens welded in each state of the water salinity. However, the potential cracks were detected only in specimens performed in freshwater (Fig. 4a). Cold cracks occurred while three factors appeared: high diffusible hydrogen content, residual stresses, and brittle microstructures [24, 29]. While one of them does not occur, the possibility of cold cracking is also limited, which suggests that water salinity has influence on the properties of welded joints, which will be checked in other tests. Moreover, it was stated that the highest number of imperfections (especially slag inclusions) was observed in specimens performed in fresh water.

In the next step, the UTPA test was performed. The exemplary photos are presented in Fig. 5. The ultrasonic scans were taken in regions, in which the biggest areas of imperfections were found in RT. Moreover, the potential cracks were scanned. UTPA showed that imperfections are observed mostly from the middle of the depth of the specimens. However, the biggest and the strongest indications are located near the root of the weld. Moreover, it was stated that increasing the water salinity provides for decreasing the size of imperfections, which confirmed results from previous RT. Specimens welded in freshwater (Fig. 5a) were characterized by bigger indications than specimens from Baltic Sea and oceanic water (Fig. 5b).

#### 3.2 Metallographic tests

In the first step, the macroscopic test was performed; exemplary macrographs are presented in Fig. 6. This test confirmed previous results. The size of observed imperfections decreased with increasing water salinity. Moreover, the strong tempering effect was observed in each specimen from the middle of the depth to the welding root. The HAZ in these regions is brighter. In our previous investigations [AS], it was proved that this effect resulted from the heat influence from beads laid on the previous stiches. However, the cracks were found in some macrographs (Fig. 6b), which are located both in the fusion line and in the weld, which is typical for cold cracking phenomenon [28]. Metallographic test also showed differences in behavior of the specimens. It was

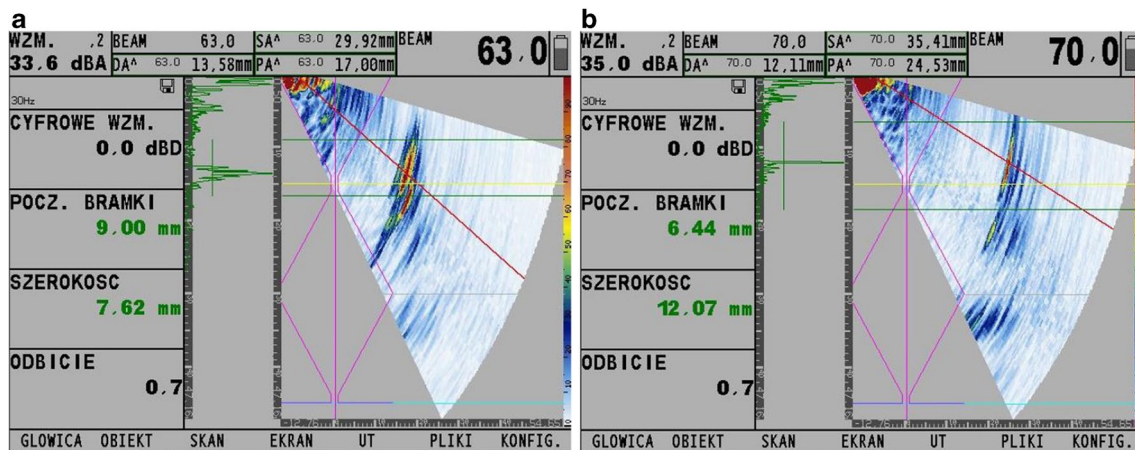


Fig. 5 Exemplary results from UTPA: **a** specimen 1—fresh water and **b** specimen 5—oceanic water

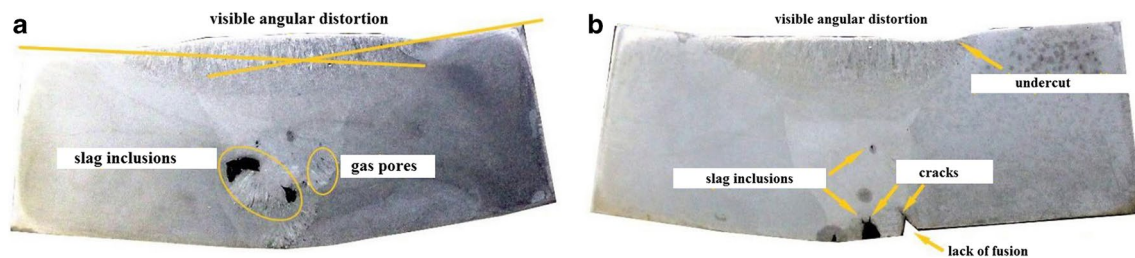


Fig. 6 Exemplary macrographs: **a** specimen 1—fresh water and **b** specimen—oceanic water

found that lower water salinity (Fig. 6a) to provide greater angular distortion of performed specimens by 30–50%. During welding in freshwater, the heat is less cumulated in the welding area following the thermal conductivity of salt water.

During microscopic test the significant effect of water salinity on the microstructure of performed joints were observed. The exemplary results of microscopic tests are presented in Fig. 7. The number of microcracks in the weld and in the HAZ decreased with increasing the water salinity. Moreover, the characteristics of cracks were different. Samples made in fresh water are characterized by presence of cracks parallel to the fusion line in the coarse-grained area of HAZ (Fig. 7a), which is typical for underwater welding [28, 29]. Additionally, cracks were observed near the root of the weld, parallel to the material surface. The shape and localization of cracks in specimens welded in Baltic Sea water were different (Fig. 7b). They were much shorter and run parallel and perpendicular to the fusion line, both in HAZ and in weld metal. The lowest number of cracks was observed in specimens welded in oceanic water (Fig. 7c). No cracks were found in the HAZ in specimens 5 and 6. Some short cracks were observed in the weld metal. The biggest differences in microstructures were noted in the middle of performed specimens. In each specimen, the tempering effect was observed both in the HAZ and in the weld. This effect resulted from the heat generated during laying

the next beads [22, 29]. The widest tempered area was observed in specimens welded in oceanic water. It can be stated that increasing the water salinity allows to increase the tempering effect. The HAZ of specimens 5 and 6 was fine-grained ferrite and pearlite compared to specimens 3 and 4 (Baltic Sea water), in which the amount of tempered martensite was found. Joints welded in fresh water are characterized by the presence of the mixed microstructure in HAZ: coarse-grained martensite (near fusion line), tempered martensite, ferrite, and pearlite near the base material. Higher water salinity allows to increase the heat concentration near the welding pool and provides for tempering the coarse-grained area of HAZ.

### 3.3 Hardness measurements

The Vickers hardness measurements were performed following the schematic draw presented in Fig. 8. Twelve measurements were performed in the HAZ, and six in the axis of the weld. Measurements were taken from the middle of the specimen's depth to the root.

The hardness measurements confirmed the results of metallographic tests. The biggest values were noticed in the specimens welded in freshwater. HAZ hardness significantly decreased with increasing the water salinity—211 HV10 for joints welded in freshwater, 198 HV10 for Baltic Sea water,

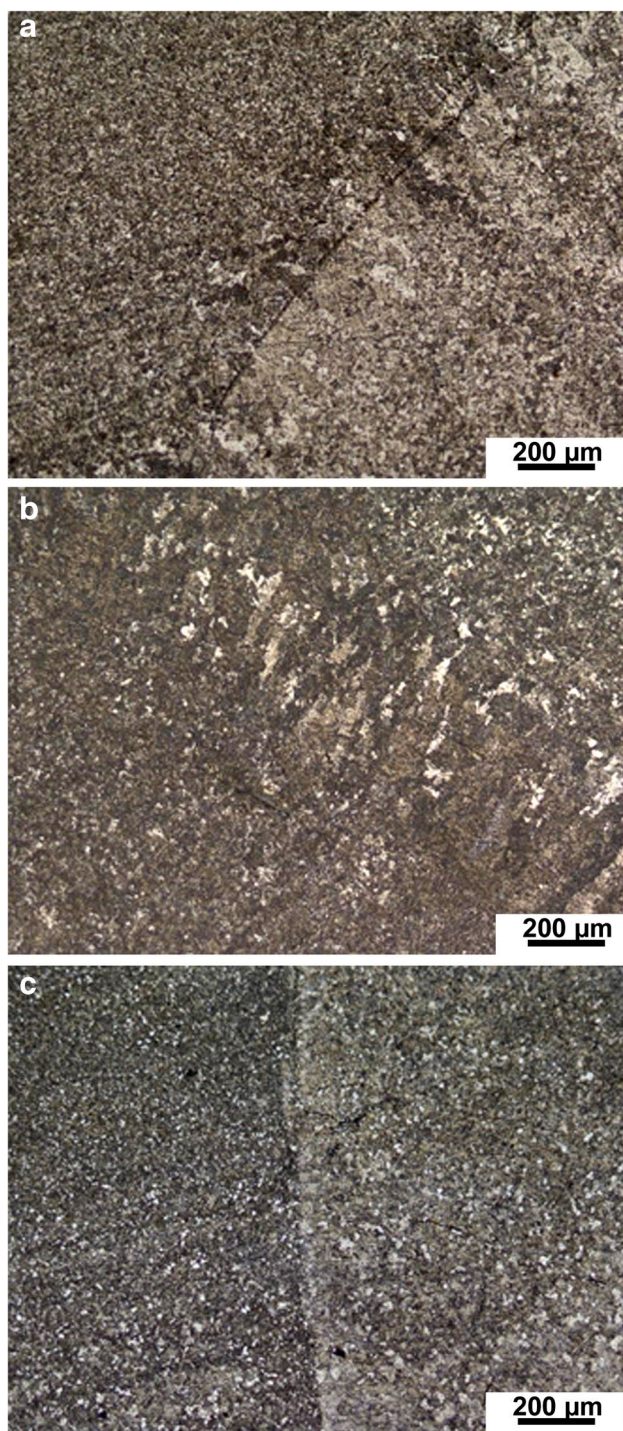


**Fig. 7** The exemplary micrographs of fusion line area: **a** specimen 1—fresh water, **b** specimen 4—Baltic Sea water, and **c** specimen 4—oceanic water

and 193 for oceanic water. Lower hardness in HAZ of HSLA steel grade suggests that susceptibility to cold cracking may be lower in higher salinity of the water environment [23, 28, 29]. Moreover, it was confirmed that the strongest tempering effect was observed in the middle of the specimens. All

results of hardness measurements are presented in Table 3. The comparison of average results with standard deviation bars are presented in Fig. 9.

### 3.4 Bending test and Charpy impact test

Similar tendencies as in previous tests were observed in the bending test and Charpy impact test. Each specimen welded in fresh and Baltic Sea water did not obtain the 180° bending angle. Aimed bending angle was achieved only for joints made in oceanic water. Higher ductility of joints made in water of higher salinity was confirmed in the Charpy impact test. Results are presented in Table 4.

The average impact strength for each state of water was calculated—82.5 J/cm<sup>2</sup> for fresh water, 94.4 J/cm<sup>2</sup> for Baltic Sea water, and 101.3 J/cm<sup>2</sup> for oceanic water. Specimens obtained under separate conditions showed different fracture modes, which is presented in Fig. 10. Specimens made in fresh water were characterized by brittle fracture. Moreover, they showed presence of porosity (Fig. 10a). Specimens made in Baltic Sea water presented less brittle fracture and lower number of imperfections (Fig. 10b). In specimens made in oceanic water, the area includes both brittle and ductile fractures (Fig. 10c). Results proved that greater number of imperfections provide lowering the mechanical properties in the state of impact load and bending. The same results were earlier observed for underwater welding [36].

### 3.5 Diffusible hydrogen content in deposited metal measurements

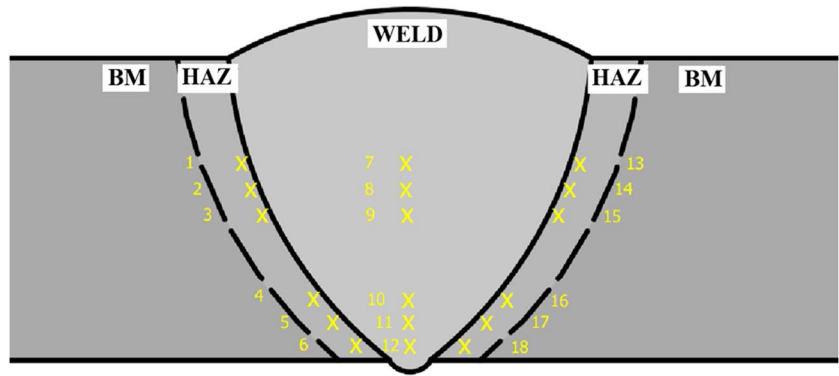
From the analysis of the average results of tests, it was concluded that higher salinity of water causes a slight increase in the diffusible hydrogen content in deposited metal from 62.1 to 65.3 ml/100g. However, from the statistical point of view, this kind of change cannot be treated as significant. In qualitative terms, obtained results are not consistent with previous information [37], but they do not change the assessment of the steel's susceptibility to cold crack formation. All results are presented in Table 5.

## 4 Conclusions

The paper presents the results of influence of the water salinity on the properties of welded joints made of S420G2+M steel by covered electrodes. As a result of this study, the following general conclusions can be drawn:

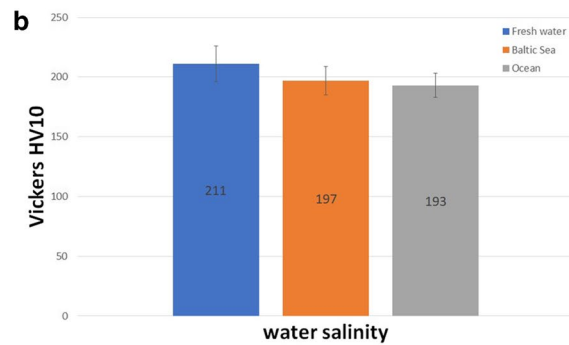
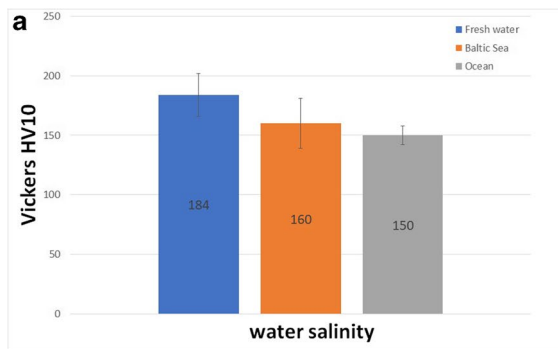
1. The level of water salinity as a welding environment affects the stability of the welding process and the properties of wet welded joints. Increased salinity

**Fig. 8** Schematic draw of the hardness measurements



**Table 3** Results of Vickers HV10 measurements

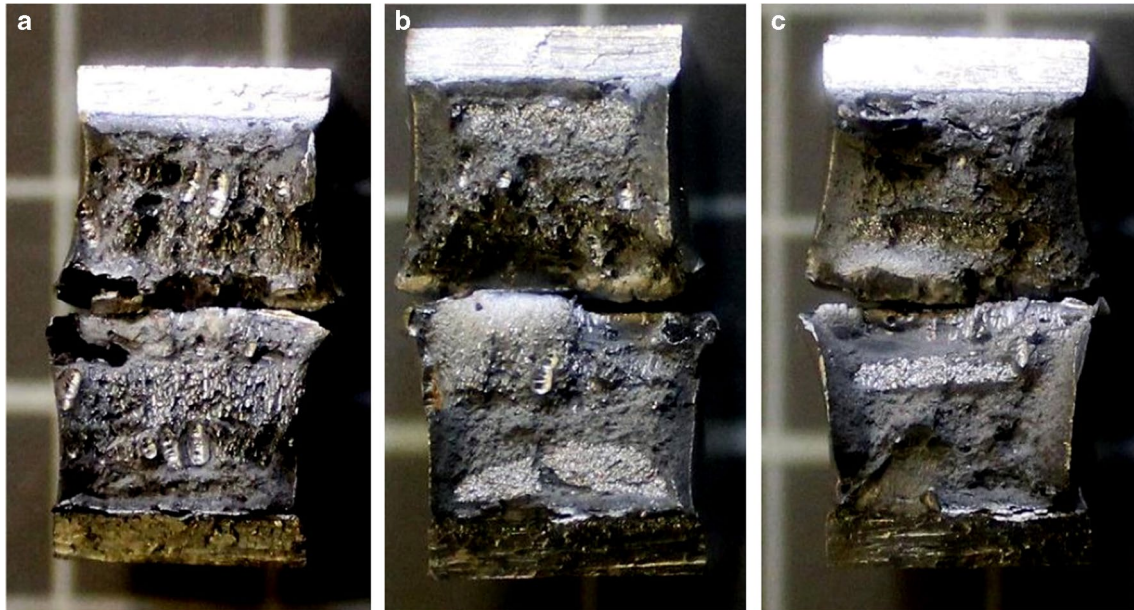
|            | Measurement point | Specimen no. |     |                  |     |               |     |
|------------|-------------------|--------------|-----|------------------|-----|---------------|-----|
|            |                   | Fresh water  |     | Baltic Sea water |     | Oceanic water |     |
|            |                   | 1            | 2   | 3                | 4   | 5             | 6   |
| HAZ        | 1                 | 182          | 190 | 184              | 190 | 195           | 190 |
|            | 2                 | 202          | 196 | 197              | 188 | 184           | 196 |
|            | 3                 | 202          | 195 | 186              | 194 | 186           | 180 |
|            | 4                 | 214          | 219 | 193              | 199 | 199           | 200 |
|            | 5                 | 232          | 227 | 199              | 208 | 209           | 204 |
|            | 6                 | 218          | 219 | 211              | 211 | 206           | 202 |
| Weld metal | 7                 | 145          | 156 | 143              | 152 | 142           | 163 |
|            | 8                 | 145          | 150 | 128              | 132 | 157           | 156 |
|            | 9                 | 149          | 162 | 129              | 130 | 150           | 158 |
|            | 10                | 192          | 175 | 150              | 184 | 159           | 172 |
|            | 11                | 182          | 169 | 138              | 182 | 168           | 163 |
|            | 12                | 198          | 184 | 149              | 186 | 169           | 168 |
| HAZ        | 13                | 199          | 208 | 161              | 192 | 181           | 181 |
|            | 14                | 195          | 206 | 199              | 190 | 179           | 178 |
|            | 15                | 197          | 198 | 190              | 187 | 181           | 183 |
|            | 16                | 225          | 224 | 211              | 211 | 195           | 197 |
|            | 17                | 232          | 216 | 217              | 200 | 208           | 205 |
|            | 18                | 250          | 218 | 212              | 208 | 193           | 202 |



**Fig. 9** Average Vickers HV10 hardness values: **a** weld metal and **b** HAZ

**Table 4** Results of Charpy impact test

|   | Specimen no. |      |                  |      |               |       |
|---|--------------|------|------------------|------|---------------|-------|
|   | Fresh water  |      | Baltic Sea water |      | Oceanic water |       |
|   | 1            | 2    | 3                | 4    | 5             | 6     |
| Impact strength (J/cm <sup>2</sup> )    | 80.0         | 85.0 | 90.7             | 98.1 | 112.8         | 110.3 |
| Average (J/cm <sup>2</sup> )            | 82.5         |      | 94.4             |      | 101.3         |       |
| Standard deviation (J/cm <sup>2</sup> ) | 2.5          |      | 3.7              |      | 1.25          |       |

**Fig. 10** Fractured area of **a** specimen 1—fresh water, **b** specimen 4—Baltic Sea water, and **c** specimen 6—oceanic water**Table 5** Results of diffusible hydrogen content in deposited metal measurements

| Type of water    | Diffusible hydrogen content Hd (ml/100g) | Average value (ml/100g) | Standard deviation (ml/100g) |
|------------------|--|-------------------------|------------------------------|
| Fresh water      | 61.08                                    | 62.06                   | 0.87                         |
|                  | 61.89                                    |                         |                              |
|                  | 63.21                                    |                         |                              |
|                  | 61.48                                    |                         |                              |
|                  | 62.65                                    |                         |                              |
| Baltic Sea water | 62.97                                    | 63.35                   | 1.04                         |
|                  | 63.44                                    |                         |                              |
|                  | 65.09                                    |                         |                              |
|                  | 62.89                                    |                         |                              |
|                  | 62.37                                    |                         |                              |
| Oceanic water    | 64.88                                    | 65.27                   | 1.01                         |
|                  | 63.77                                    |                         |                              |
|                  | 66.21                                    |                         |                              |
|                  | 65.34                                    |                         |                              |
|                  | 66.15                                    |                         |                              |

resulted in more stable welding arc, which improves welding process and quality of welded joints.

2. Hardness of HAZ of joints made in oceanic water decreased by 15–20 HV10 compared to joints welded in freshwater.
3. Water salinity of the water environment affects the impact strength. Specimens welded in fresh water are characterized by average 82.5 J/cm<sup>2</sup>. Baltic Sea water allows to get impact strength 94.4 J/cm<sup>2</sup>, and oceanic water 110.3 J/cm<sup>2</sup>.
4. The tempering effect during multipass welding depends on the water salinity. Higher water salinity allows to increase the heat concentration near the welding pool, and provides for tempering the coarse-grained area of HAZ.
5. Increasing the water salinity resulted in slight, but statistically insignificant, increasing the diffusible hydrogen content in deposited metal by 3 ml/100g to a level of 65 ml/100g.



## Declarations

**Conflict of interests** The authors declare no competing interests.

**Open Access** This article is licensed under a Creative Commons Attribution 4.0 International License, which permits use, sharing, adaptation, distribution and reproduction in any medium or format, as long as you give appropriate credit to the original author(s) and the source, provide a link to the Creative Commons licence, and indicate if changes were made. The images or other third party material in this article are included in the article's Creative Commons licence, unless indicated otherwise in a credit line to the material. If material is not included in the article's Creative Commons licence and your intended use is not permitted by statutory regulation or exceeds the permitted use, you will need to obtain permission directly from the copyright holder. To view a copy of this licence, visit <http://creativecommons.org/licenses/by/4.0/>.

## References

- Zhang X, Hao F, Zhang Y, Li X, Guo H (2022) Corrosion behavior and mechanism of the high-strength low-alloy steel joined by multilayer and multipass welding method. *Mater Corros* 73(11):1826–1832. <https://doi.org/10.1002/maco.202213154>
- Guo T, Shao Y, Gao X, Li T, Zhong T, Luo L (2022) Corrosion fatigue crack growth of serviced API 5L X56 submarine pipeline. *Ocean Eng* 256:111502. <https://doi.org/10.1016/j.oceaneng.2022.111502>
- Moreno-Urbe AM, Bracarense AQ, Pessoa ECP (2020) The effect of polarity and hydrostatic pressure on operational characteristics of rutile electrode in underwater welding. *Materials* 13:5001. <https://doi.org/10.3390/ma13215001>
- Wang J, Ma J, Liu Y, Zhang T, Wu W, Sun Q (2020) Influence of heat input on microstructure and corrosion resistance of underwater wet-welded E40 steel joints. *J Mater Eng Perform* 29:6987–6996. <https://doi.org/10.1007/s11665-020-05160-7>
- Ma Q, Li H, Liu S, Liu D, Wang P, Zhy Q, Lei Y (2022) Comparative evaluation of self-shielded flux-cored wires designed for high strength low alloy steel in underwater wet welding: arc stability, slag characteristics, and joints' quality. *J Mater Eng Perform* 31:5231–5244. <https://doi.org/10.1007/s11665-022-06683-x>
- Chen J, Wen Z, Jia C, Zhao B, Wu CS (2022) The mechanisms of underwater wet flux-cored arc welding assisted by ultrasonic frequency pulse high-current. *J Mater Process Technol* 304:117567. <https://doi.org/10.1016/j.jmatprotec.2022.117567>
- Treutler K, Brechtel S, Wiche H, Wesling V (2022) Beneficial use of hyperbaric process conditions on the welding of high-strength low alloy steels. *Sci Rep* 12:12434. <https://doi.org/10.1038/s41598-022-16184-5>
- Guro I, Baykal H, Yildiz NB, Yilmaz C, Daniskan O, Kocak M (2022) Investigation of the microstructural and mechanical properties of welding joints made with underwater electrodes. *J Fac Eng Archit Gazi Univ* 37:2211–2223. <https://doi.org/10.17341/gazimmfd.990465>
- Hu Y, Shi Y, Wang K, Huang J (2023) Effect of heat input on the microstructure and mechanical properties of local dry underwater welded duplex stainless steel. *Materials* 16:2289. <https://doi.org/10.3390/ma16062289>
- Fydrych D, Raczko P, Świerczyńska A, Landowski M, Wolski A, Rogalski G (2023) Effect of arc strikes on high strength low alloy steels welded by SMAW. *Adv Sci Technol Res J* 17(3):160–169
- Wang J (2023) Finite-element analysis of underwater wet welding: implementation of bubble configuration. *Weld J* 102:97s–112s. <https://doi.org/10.29391/2023.102.008>
- Wang J, Li H, Hu C, Wang Z, Han K, Liu D, Wang J, Zhu Q (2023) The efficiency of thermite-assisted underwater wet flux-cored arc welding process: electrical dependence, microstructural changes, and mechanical properties. *Metals* 13:831. <https://doi.org/10.3390/met13050831>
- Sisodia RPS, Gaspar M (2021) Experimental assessment of microstructure and mechanical properties of electron beam welded S960M high strength structural steel. *Manuf Lett* 29:108–112. <https://doi.org/10.1016/j.mfglet.2021.05.004>
- Zhang LF, Wang YF, Zhang L, Wang QF, Wang TS (2022) Mo content effect on microstructures and toughness of the simulated coarse-grained heat-affected zone of weathering bridge steels. *J Mater Eng Perform* 31:5641–5651. <https://doi.org/10.1007/s11665-022-06687-7>
- Wang ZW, Liu M, Zhang H, Xie GM, Xue P, Wu LH, Zhang Z, Ni DR, Xiuo BL, Ma ZY (2022) Welding behavior of an ultrahigh-strength quenching and partitioning steel by fusion and solid-state welding methods. *J Mater Res Technol* 17:1289–1301. <https://doi.org/10.1016/j.jmrt.2022.01.086>
- Mičian M, Winczek J, Harmaniak R, Koňár R, Gucwa M, Moravec J (2021) Physical simulation of individual heat-affected zones in S960MC steel. *Arch Metall Mater* 66(1):81–89. <https://doi.org/10.24425/amm.2021.134762>
- Szymczak T, Szczucka-Lasota B, Węgrzyn T, Łazarz B, Jurek A (2021) Behavior of weld to S960MC high strength steel from joining process at micro-jet cooling with critical parameters under static and fatigue loading. *Materials* 14(11):2707. <https://doi.org/10.3390/ma14112707>
- Branco R, Martins RF, Correia JAFO, Marciniak Z, Macek W, Jesus J (2022) On the use of the cumulative strain energy density for fatigue life assessment in advanced high-strength steels. *Int J Fatigue* 164:107121. <https://doi.org/10.1016/j.ijfatigue.2022.107121>
- Kumar SN, Balasubramanian V, Malarvizhi S, Rahman AH, Balaguru V (2022) Effect of welding consumables on shielded metal arc welded ultra high hard armour steel joints. *J Mech Behav Mater* 31:8–21. <https://doi.org/10.1515/jmbm-2022-0002>
- Majlinger K, Katula LV, Varbai B (2022) Prediction of the shear tension strength of resistance spot welded thin steel sheets from high- to ultrahigh strength range. *Period Polytech Mech Engrg* 66:67–82. <https://doi.org/10.3311/PPme.18934>
- Skowrońska B, Szulc J, Bober M, Baranowski M, Chmielewski T (2022) Selected properties of RAMOR 500 steel welded joints by hybrid PTA-MAG. *J Adv Join Process* 5:100111. <https://doi.org/10.1016/j.jajp.2022.100111>
- Tomków J, Landowski M, Fydrych D, Rogalski G (2022) Underwater wet welding of S1300 ultra-high strength steel. *Mar Struct* 81:103120. <https://doi.org/10.1016/j.marstruc.2021.103120>
- Brätz O, Klett J, Wolf T, Henkel KM, Maier HJ, Hassel T (2022) Induction heating in underwater wet welding—thermal input, microstructure and diffusible hydrogen content. *Materials* 5:1417. <https://doi.org/10.3390/ma15041417>
- Tomkow J, Fydrych D, Rogalski G (2020) Dissimilar underwater wet welding of HSLA steels. *Int J Adv Manuf Technol* 109:717–725. <https://doi.org/10.1007/s00170-020-05617-y>
- Klett J, Hecht-Linowitzki J, Grünzel O, Schmidt E, Maier HJ, Hassel T (2020) Effect of the water depth on the hydrogen content in SMAW wet welded joints. *SN Appl Sci* 2:1269. <https://doi.org/10.1007/s42452-020-3066-8>
- Fydrych D, Świerczyńska A, Tomków J (2013) Diffusible hydrogen control in flux cored arc welding process. *Key Eng Mater* 597:171–178. <https://doi.org/10.4028/www.scientific.net/KEM.597.171>
- Tomków J, Landowski M, Rogalski G (2022) Application possibilities of the s960 steel in underwater welded structures. *Facta Universitatis Series. Mech Eng* 20:199–209. <https://doi.org/10.22190/FUME210722066T>

28. Tomków J (2021) Weldability of underwater wet-welded HSLA steel: effects of electrode hydrophobic coatings. *Materials* 14:1364. <https://doi.org/10.3390/ma14061364>
29. Tomków J, Rogalski G, Fydrych D, Łabanowski J (2018) Improvement of S355G10+N steel weldability in water environment by temper bead welding. *J Mater Process Technol* 262:372–381. <https://doi.org/10.1016/j.jmatprotec.2018.06.034>
30. Nthunya LN, Bopape MF, Mahlangu OT, Mamba BB, Van der Bruggen B, Quist-Jensen CA, Richards H (2022) Fouling, performance and cost analysis of membrane-based water desalination technologies: a critical review. *J Environ Manage* 301:113922. <https://doi.org/10.1016/j.jenvman.2021.113922>
31. Kononenko VY (1989) Effect of water salinity and mechanized underwater welding parameters on hydrogen and oxygen content of weld metal. In: *Proceedings of the International Conference Welding Under Extreme Conditions*, pp 113–119
32. Fydrych D, Rogalski G (2011) Effect of shielded-electrode wet welding conditions on diffusion hydrogen content in deposited metal. *Weld Int* 25(3):166–171. <https://doi.org/10.1080/09507116.2010.540828>
33. Yushchenko KA, Gretsikii YY, Maksimov SY (1998) Study of physio-metallurgical peculiarities of wet arc welding of structural steels. In: *Underwater Wet Welding and Cutting*, pp 6–29. <https://doi.org/10.1533/9780857093165.6>
34. Klett J, Wolf T, Maier HJ, Hassel T (2020) The applicability of the standard DIN EN ISO 3690 for the analysis of diffusible hydrogen content in underwater wet welding. *Materials* 13(7):3750. <https://doi.org/10.3390/ma13173750>
35. Xu S, Han Y, Jia C, Maksymov S, Kakhovskyi M, Wu C (2022) Numerical modeling of coupled arc plasma, metal transfer and molten pool evolution for underwater flux-cored arc welding. *Int J Adv Manuf Technol* 123(7):2605–2622. <https://doi.org/10.1007/s00170-022-10367-0>
36. Tomków J, Janeczek A, Rogalski G, Wolski A (2020) Underwater local cavity welding of S460N steel. *Materials* 13:5535. <https://doi.org/10.3390/ma13235535>
37. Świerczyńska A, Fydrych D, Rogalski G (2017) Diffusible hydrogen management in underwater wet self-shielded flux cored arc welding. *Int J Hydrog Energy* 42(38):24532–24540. <https://doi.org/10.1016/j.ijhydene.2017.07.225>

**Publisher's note** Springer Nature remains neutral with regard to jurisdictional claims in published maps and institutional affiliations.